Performance Testing of a Hybrid Imitation Learning and Rule-Based Approach for Real-Time Microgrid Energy Management

Taheni Swibki*, Dhaker Abbes, Kais Ouni*, Lilia El Amraoui*****

** Research Laboratory Smart Electricity & ICT, National Engineering School of Carthage, University of Carthage, Tunisia,*
(taheni.swibki@enicar.ucar.tn, kais.ouni@enicar.ucar.tn)
*** Univ. Lille, Arts et Metiers Institute of Technology, Centrale Lille, Junia, ULR 2697–L2EP, F-59000 Lille, France, (dhaker.abbes@junia.com)*
****Department of Electrical Engineering, College of Engineering, Princess Nourah bint Abdulrahman University, P.O. Box 84428, Riyadh 11671, Saudi Arabia, (LEOuni@pnu.edu.sa)*

Abstract: This paper investigates a hybrid approach that combines Imitation Learning (IL) and rule-based methods for real-time energy management in a full-scale, grid-connected microgrid (MG). This approach eliminates the need for forecasting models, which can be complex and unreliable. The primary objective of this method is to minimize energy costs by reducing dependence on the external grid through optimal control of the storage system and photovoltaic (PV) power generation of the Lille Catholic University demonstrator. The proposed method integrates a Deep Learning (DL) model trained to mimic the behavior of a Linear Programming (LP)-based energy management strategy. The optimal control outputs of the LP, derived from real historical data, serve as training demonstrations for the IL process. This enables the DL model to learn how to replicate optimal energy management decisions. Since DL models cannot inherently enforce operational constraints (e.g., storage limits, energy balance, etc.), a rule-based post-processing module is used to ensure that the microgrid operates within its operational limits. Numerical experiments demonstrate the effectiveness of the proposed method in enhancing responsiveness and efficiency in real-time energy management.

Keywords: Real-Time Energy Management, Microgrid Optimization, Imitation Learning, Rule-Based Control, Deep Learning.

1. INTRODUCTION

Energy is considered the essence of life and the driving force behind economic growth and technological advancement, powering everything from basic daily needs such as transportation, lighting, and heating to advanced technologies. (U.S. energy information administration n.d.). Fossil fuels have been and continue to be the dominant source of energy in the world (Wang and Azam, 2024). However, reliance on fossil fuels leads to critical issues, particularly in terms of energy equity, security, and sustainability. Therefore, developing a new energy matrix that integrates clean energy to ensure a reliable, cost-effective, and decarbonized power supply has become a matter of global concern (Erdiwansyah et al., 2021).

The large-scale deployment of renewable energy generators puts additional strain on the power system, triggering stability issues due to uncertainties in demand and supply (Brahmendra Kumar et al., 2019). As highlighted by (Zhou and Ho., 2016), to minimize the impact of renewable energy on the power system, the integration of microgrids (MGs) emerges as an effective solution when properly controlled. The control strategy of a MG ensures optimal operation to achieve economic, technical, and environmental objectives while maintaining system stability, efficiency, and security (Kruse et al., 2021; Hanley et al., 2011; Uddin et al., 2023).

In this context, the implementation of an Energy Management System (EMS) in the MG control architecture is essential for optimal resource exploitation and integration into the power system (Uddin et al., 2023; Ahmadifar et al., 2023). As outlined by the IEC 61970 standard, an EMS is a software platform offering core support services with applications designed to ensure the efficient operation of electrical generation and transmission systems that aim to maintain energy supply at minimal cost (Vinothine et al., 2022). Analogously, a microgrid EMS (MG-EMS) is software developed to execute decision-making strategies that ensure coordinated control and optimize energy allocation.

Forecasting is a key component of energy management strategies, predicting critical factors such as demand, supply, and pricing. It is widely employed across all industry segments, providing essential input for energy management and planning (Hong et al., 2020). Short-term energy forecasting helps anticipate future trends, detect stability issues, prevent overloading, and support sustainability (Mystakidis et al., 2024). While most energy management approaches rely on forecasting, predicting outputs from intermittent energy sources is particularly challenging. Inaccurate forecasts can disrupt energy management, leading to inefficiencies, increased costs, and suboptimal energy allocation (Boralessa et al., 2022).

Due to the rapid expansion of artificial intelligence and the exponential growth of data, more advanced data-driven energy management methods have gained significant attention. Unlike traditional approaches, these methods can operate effectively without relying on energy forecasting (Gao et al., 2024; Sun et al., 2023; Ji et al., 2019; Boato et al., 2023).

One of these methods is Imitation Learning (IL), where an agent learns a task by imitating expert demonstrations, which enables it to learn complex decision-making strategies (Zare et al., 2024). Numerous studies in the literature have explored breakthroughs in IL for energy management in MGs while ignoring the dependence on forecasting models. Particular focus is given to the work by (Gao et al., 2022) , as it is closely related to our study. In this work, the authors proposed an IL-based approach replicating the performance of a Mixed-Integer Linear Programming (MILP) to control a storage system. Since DL models cannot inherently learn to maintain complex physical constraints such as power balance, storage limits, etc, a one-step MILP was used subsequently to maintain the MG constraints and compute other setpoints. This hybrid approach achieved a near-optimal performance with improved computational efficiency.

Building on this concept, this study tests a real-time IL-based approach on a full-scale MG system: the Lille Catholic University Smart Grid Demonstrator. A DL model is trained to mimic an LP model using reference demonstrations, which consist of MG states and their corresponding actions, obtained by solving a set of LP problems based on historical real data. After training, the DL model can operate in real-time to compute setpoints for the system components. A rule-based algorithm serves as a post-processing block to enforce the MG constraints. This real-time capability is considered a significant advancement, allowing adaptive energy management without depending on predictive forecasts.

This article is structured as follows: A full-scale case study is described in section 2. In section 3, the corresponding energy management problem is formulated as an LP problem, considering PV power curtailment and zero-grid-injection conditions. In section 4, an innovative approach based on IL is proposed. The simulation results of this approach are presented in section 5. Finally, conclusions and perspectives are discussed in section 6.

2. CASE STUDY DESCRIPTION: LILLE CATHOLIC UNIVERSITY DEMONSTRATOR

A full-scale MG at the Lille Catholic University is used as a case study to later test the effectiveness of the proposed energy management approaches. The demonstrator is located in the heart of the “Quartier Vauban” in Lille, France. Figure 1 depicts a top view of the site from Google Earth, showing its architecture in detail, while Fig. 2 shows its electrical model.

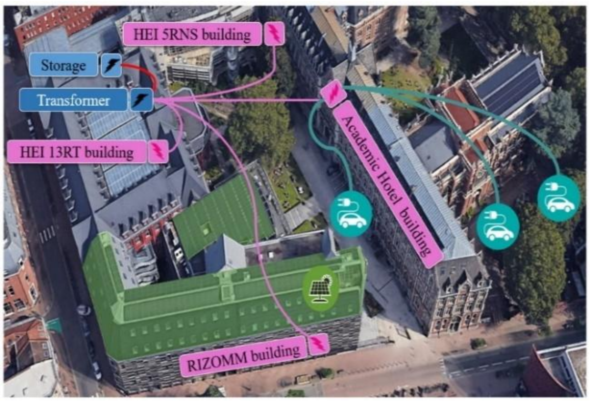

Fig. 1. Lille Catholic University smart grid demonstrator (Swibki et al., 2023).

The system is composed of two PV systems, four buildings, a storage system, an electric vehicle charging station, and a point of common coupling to the distribution grid through a 1 MVA 15 kV/0.4 kV transformer. The first PV system, installed on the RIZOMM building, was deployed on a 1200 m2 area and produces 189 kWp. The second PV system is installed on the rooftop of the HEI 13RT building and produces 28 kWp. The two systems are interfaced to the grid via 12 Fronius inverters. Excess PV power is stored in a Li-ion Eaton xStorage system of 250 kWh installed in the basement of the HEI building and connected to the grid through two inverters. The electric vehicle charging station is composed of six charging points at 22 kW each point. However, these charging points are not considered in the present study.

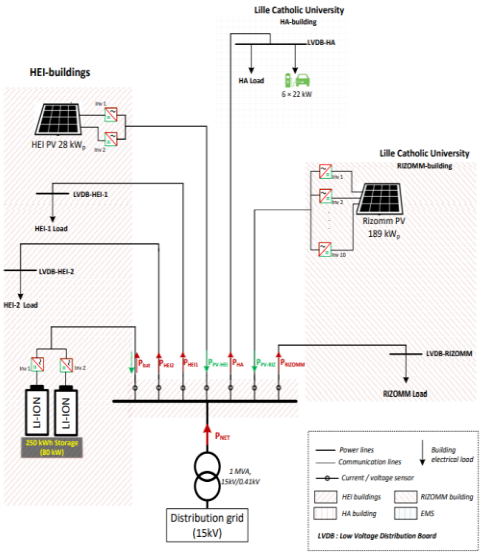

Fig. 2. Diagram of the Lille Catholic University demonstrator (Aouad et al., 2024).

In this study, since we are investigating energy management, the following power flows are considered:

- Grid power $P_g(t)$: the power flow between the campus and the distribution grid, where $P_g(t) > 0$ when pulling power from the grid, otherwise $P_g(t) = 0$.
- PV power $P_{PV}(t)$: aggregated power produced by the two PV systems.
- Battery power $P_b(t)$: the power flow of the storage system, it is charging if $P_b(t) > 0$, discharging if $P_b(t) < 0$ and Idle when $P_b(t) = 0$.
- Power demand $P_{load}(t)$: the aggregated consumption of the four academic buildings.

3. ENERGY MANAGEMENT PROBLEM FORMULATION

3.1 Objective

In this study, the main objectives of the energy management problem are to minimize dependence on the external grid, promote local power generation, and maintain the MG's operational constraints. These objectives are formulated as an LP problem, involving a linear objective function in combination with a set of linear constraints. Below is the detailed formulation of the studied problem.

3.2 Objective function

The objective function, expressed in (1), minimizes the cost of energy imported from the external grid over a defined time horizon, generally 24 hours. This is achieved by reducing reliance on imported energy during peak periods and optimizing the use of local energy resources.

$$J = min \sum_{t=1}^{T} \left(P_g(t) * C(t) * \Delta t\right) \quad (1)$$

where C(t) denotes the electricity price, $P_g(t)$ represents the power drawn from the external grid, T corresponds to the time horizon of the problem, and Δt is the decision time step.

3.3 Operational constraints

The dynamic evolution of the Li-ion battery is expressed in (2). This model is fundamental as it enables the monitoring of the battery's energy level at every decision step, ensuring efficient operation of the system.

$$E_{bat}(t) = E_{bat}(t-1) + P_b(t) * \Delta t \quad (2)$$

where $E_{bat}(t-1)$ is the previous energy level.

Overcharging and overdischarging Li-ion batteries can significantly affect their lifespan and performance by causing structural damage and irreversible chemical degradation (Ouyang et al., 2022; Kim and Shin 2023). The role of the EMS is to mitigate these phenomena. Thus, the following constraints prevent the battery from overcharging and overdischarging:

$$E_{batmin} \le E_{bat}(t) \le E_{batmax} \quad (3)$$

where E_{batmin} is the minimum energy level in the battery below which discharging is restricted and E_{batmax} is the maximum energy level which is restricted to avoid overcharging.

For the same reasons, limits on the charging and discharging rates are defined:

$$P_{Dis}^{max} \le P_b(t) \le P_{Ch}^{max} \quad (4)$$

where P_{Ch}^{max} is the maximum charge rate and P_{Dis}^{max} is the maximum discharge rate.

For the particular scenario of the Catholic University Smart Grid demonstrator, it is imperative that the power produced by the local PV system must be entirely consumed by local loads, with no excess power allowed to be injected to the external grid (Aouad et al., 2024). Additionally, the imported power is limited to a predefined limit P_g^{max}. Thus, the following constraint is defined:

$$0 \le P_g(t) \le P_g^{max} \quad (5)$$

To prevent power injection into the external grid, excess PV power is curtailed. According to (6), any PV power exceeding the load demand and the available battery charging capacity must be curtailed. On the other hand, the curtailed power must not exceed the available power as expressed in (7).

$$P_{curt}(t) \ge P_{PV}(t) - P_{load}(t) - max(0, P_b(t)) \quad (6)$$

$$P_{curt}(t) \le P_{PV}(t) \quad (7)$$

By enforcing the previous curtailment constraints, excess PV power is used to charge the battery, otherwise it is cut off from the system via inverters control.

The power balance is a fundamental constraint to ensure the stable and reliable operation of a power system by a proactive balance of supply and demand (Aslam et al., 2021). For a grid-connected MG, power produced by local generators, power charged/discharged by the battery, and power exchanged with the external grid must be equal to the demand at every time step. The power balance condition is mathematically formulated as follows:

$$P_{PV}(t) - P_{curt}(t) + P_b(t) + P_g(t) = P_{load}(t) \quad (8)$$

4. IL-BASED ENERGY MANAGEMENT APPROACH

4.1 Principle

IL is defined as "socially inspired" machine learning paradigm, allowing an agent to learn a skill or a behavior by observing and replicating a teacher (expert) executing a given task (Aslam et al., 2021). These demonstrations are typically composed of state-action pairs, where states represent the environment (context), while actions capture the expert behavior (decisions) in these states.

The central idea of the present work is to reframe the energy management problem, defined in Section 3, as an IL problem. The proposed approach, depicted in Fig. 3, leverages the performance of LP-based optimization in solving the energy management problem to generate demonstrations that will be used to train an agent. Behavioral cloning (BC), the simplest form of IL, is applied in this work. This approach reduces the IL problem to a simple Supervised Learning (SL) problem, enabling the agent to learn how to map states to actions based on expert demonstrations (Chen et al., 2024).

4.2 State-action representation

To make well-informed decisions, the IL-agent must construct an accurate representation of the MG environment. This representation is formed by continuously perceiving the MG's state at every decision step. The MG state includes key operational variables that model the MG's dynamics. In this study, the MG is represented at each decision step by its state, which is defined by the state representation in (9). These parameters are assumed to be sufficient to fully capture the MG's state.

$$S_t = \{P_{PV}(t), P_{load}(t), \ E_{bat}(t), C(t), hour\} \quad (9)$$

In this study, the IL agent makes control decisions that influence the MG power flow while meeting the objectives of the energy management problem. The actions are defined by the following action representation.

$$A_t = \{P_{curt}(t), P_b(t)\} \quad (10)$$

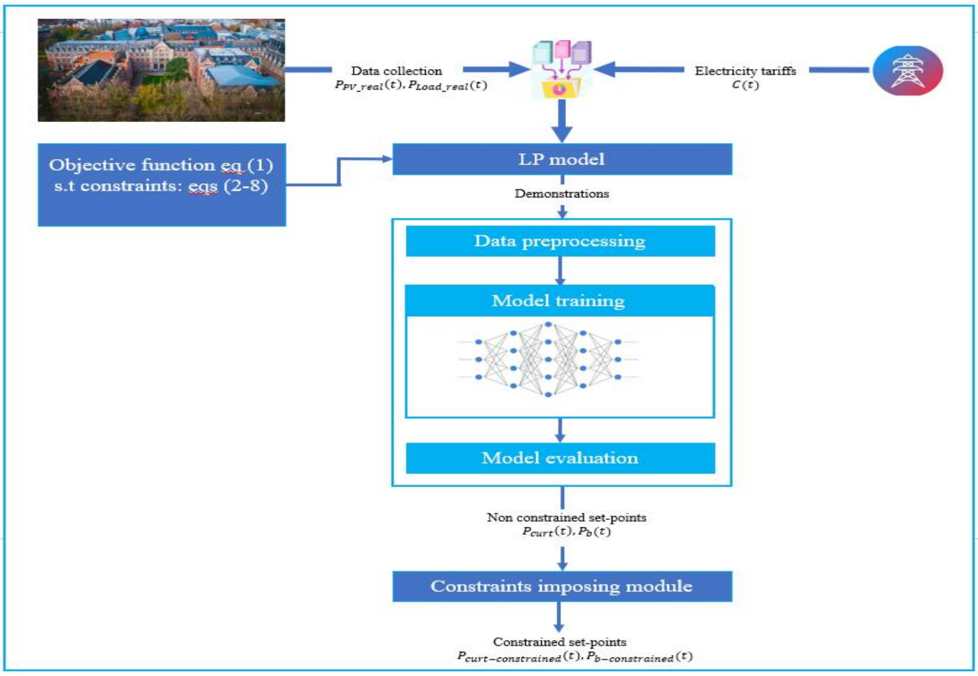

Fig. 3. Schematic of IL-based decision-making for MG energy management.

4.3 Data generation

As depicted in Fig. 3, the MG's PV generation, consumption patterns and pricing data are fed into an LP model to generate the state-action pairs defined previously. The data used in the simulation are sourced from a real-world dataset containing historical time-series data from the Catholic University. This dataset includes PV power, consumption patterns, and their corresponding time steps. It is sampled at a 1-hour time step from January 1, 2020, to May 30, 2020, resulting in 3648 samples. The pricing data is constructed to align with the number of samples, following a time-of-use (ToU) policy, which is detailed later in the simulation setup section. These inputs are processed by the LP model, formulated in Section 3, to derive the battery energy levels and the control actions of the battery and the PV system. The resulting state-action pairs serve as 'ground-truth' data for a SL model. The following pseudocode summarizes how the demonstrations were generated.

Pseudocode 1: Demonstration Data Generation

1. Load input data: $Ppv(t), Ploads(t), C(t)$ where $t \in \{1, \ldots, T\}$
2. Generate expert demonstrations using the LP Model:
   For time step t = 1 to T do:
      a. Solve the LP problem (Eq. 1-8) using input data
      b. Extract the optimal setpoints: $P_{curt}(t), P_b(t)$
   End for.
3. Construct the demonstration dataset by storing each state with its corresponding optimal action:
   - states = $\{P_{PV}(t), P_{load}(t), E_{batt}(t), C(t), hour\}$
   - action = $\{P_{curt}(t), P_b(t)\}$

4.4 Supervised Learning

A Deep Neural Network (DNN) model is employed to learn mapping states to actions, imitating the behaviour of the LP model. The DNN model is implemented as a Feed Forward Neural Network (FNN) composed of an input layer corresponding to input data, three hidden layers composed of 128, 64 and 32 neurons for features extraction, two dropout layers to prevent overfitting, and an output layer composed of the output data. This architecture enables the DNN model to approximate the optimal control strategy derived from LP while maintaining robustness and generalization capabilities. The operation of the IL-based approach is depicted in the following Pseudocode.

Pseudocode 2: Supervised model training

Input:
- features: X=$\{P_{PV}(t), P_{load}(t), E_{batt}(t), C(t), hour\}$
- Target : Y= $\{P_{curt}(t), P_b(t)\}$
Output:
- Trained policy
1. Data-preprocessing
   b. Split the dataset into training and testing subsets.
   c. Normalize both input and target data using standard
      scaling.
2. Build the DNN architecture
3. Compile the DNN model:
   - Optimizer: RMSprop
   - Loss function: Mean Squared Error (MSE)
4. Train the model using the pre-processed training data according to number of epochs and batch size
5. Evaluate the trained model on the test data
6. Return the trained policy
7. Apply the trained policy to predict actions on new data

4.5 Constraint Imposing post-processing module

To apply the learned policy in real-time conditions, a rule-based constraint-imposing module based on the system operational limits defined in (2)–(8) is used. This module ensures that the output set-points of the derived policy from the DNN model are restricted within the system operational constrained defined in Section 3.

Pseudocode 3: Constraint Imposing post-processing module

Input: $P_{curt}(t), P_b(t)$
Output: $P_{curt-constrained}(t), P_{b-constrained}(t)$
1. Apply limit constraints on inputs
2. check and maintain power balance:
    b- compute power balance
    a- If power balance <0: (excess power)
        - Try to charge the battery if possible
        - If imbalance remains:
            - increase PV curtailment
    b- Else: (power balance > 0 : power deficit)
        - Discharge more the storage if possible,
        - If imbalance remains:
            - reduce curtailment
                - If imbalance remains:
                    -increase grid import
Return corrected setpoints: $P_{curt-constrained}(t)$, $P_{b-constrained}(t)$

5. SIMULATION RESULTS

5.1 Simulation setup

The Catholic University smart grid demonstrator, described in Section 2, serves as a realistic case study for conducting an in-depth analysis and testing of the proposed energy management approach. All simulations were executed on Google Colab, with Table 1 providing the technical parameters used. This study aims to replicate the performance of the LP-based optimization to solve the predefined energy management problem. Notably, this approach is applied in real-time, eliminating the need for forecasting system variables (PV power, consumption, and pricing).

Table 1. Simulation parameters.

Parameter	Value
Battery capacity	$C = 250\ kWh$
Max charging rate	$P_{ch}^{max} = 40\ kW$
Max discharging rate	$P_{Dis}^{max} = 80\ kW$
Max battery energy level	$E_{batmax} = 0.9 * C$
Min battery energy level	$E_{batmin} = 0.1 * C$
Max grid import limit	$P_g^{max} = 580\ kW$

The simulation setup consists of two models: an LP model and an IL model. The LP model, implemented using Python on Google Colab, formulates the energy management problem as a LP problem based on (1)–(8) via the pulp.LpProblem library. The objective of this approach is to minimize operational costs by optimally controlling the battery charging and discharging rates, as well as the amount of PV power curtailment. These control setpoints are used as targets outputs for training the IL model, alongside historical data from the catholic university.

For the purpose of this study, a ToU pricing model, in which electricity tariffs vary depending on the time of day, is implemented in the simulations. A hypothetical ToU pricing scheme, outlined in Table 2, is assumed to analyze the performance of the proposed method.

Table 2. Electricity Tariffs by Period

Period	Time	Tariff
Off-peak	22:00-06:00	0.08 £/kWh
Mid-peak	06:00–09:00	0.12 £/kWh
	18:00–22:00	
Peak	09:00–18:00	0.18 £/kWh

Figure 4 illustrates the PV production and load patterns over five months in 2020. In a real-world setting, the Catholic University experiences a higher aggregated load demand compared to PV production of both systems. To address this, the data was rescaled to ensure more days with higher PV generation, thereby enhancing the model's ability to handle various real-world scenarios. This data is then used to generate training data for the DNN model.

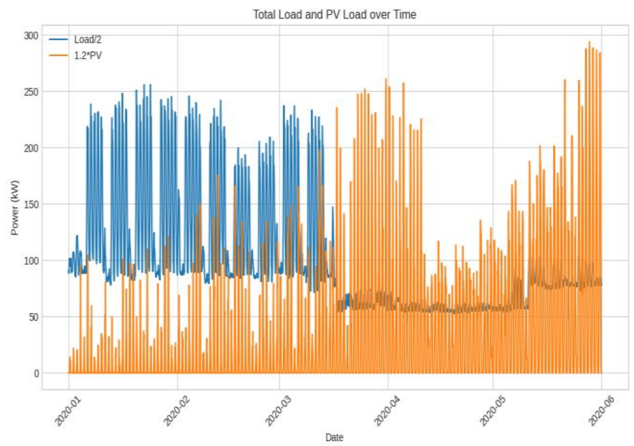

Fig. 4. rescaled energy consumption and generation data from January to May 2020.

Two test scenarios are designed to evaluate the studied approach's ability to adapt to different conditions:

- Scenario 1: reproduces a sunny day with high PV power generation.
- Scenario 2: replicates a cloudy day with significantly reduced PV power due to weather conditions.

In both scenarios, the load pattern is assumed to be identical.

5.2. Simulation results

Figure 5 shows the evolution of the training and validation losses over 80 epochs. Both curves decrease to low values, with the validation loss closely tracking the training loss. The absence of divergence between the two losses and convergence to low values rules out overfitting and underfitting. Consequently, the training process indicates effective learning and strong generalization.

In order to analyse the performance of the DNN model, the metrics in table 3 are employed, where MAE is defined as the Mean Absolute Error, RMSE stands for the Root Mean Square Error, and R^2 is the coefficient of determination, which is used to evaluate the performance of a DNN models in regression tasks. It measures how well the model approximates the target values when compared to a simple baseline that predicts the mean of the target values.

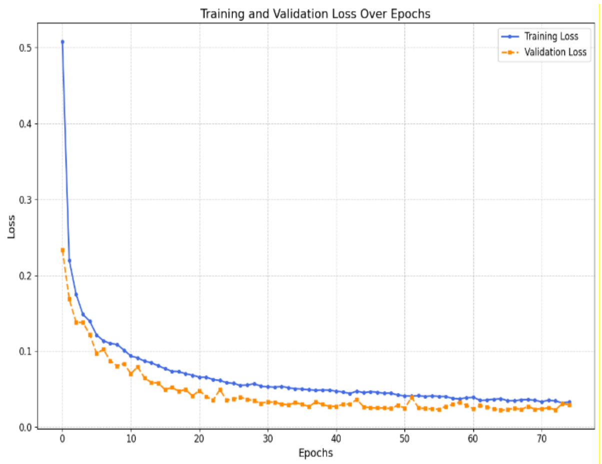

Fig. 5. Evolution of the training and validation losses.

Based on these defined metrics, the model demonstrates promising predictive performance. The MAE shows a small deviation between predicted and ground-truth values, while the MSAE shows a larger margin, however, it remains within an acceptable range. Notably, the R2 shows the ability of the model to make accurate predictions. The Validation loss and the training loss over the test dataset show that the model has learned effectively from data and has a good generalization to unseen data.

Table 3. Simulation performance metrics.

Metric	Value
MAE	1.84
RMSE	4.76
R^2	97.86%
Training loss	0.0341
Validation loss	0.0291

Alongside the previously defined metrics, Fig. 6 illustrates the predictions made on the test data. The test data are considered as ground truth values, derived from the LP model. Notably, the general trend of predicted values closely aligns with the real data, demonstrating the model's performance in replicating the general trend of the data accurately.

Simulations conducted over a 24-hour period, depicted in Fig. 7 and Fig. 8, show the results of applying the proposed approach in test scenarios 1 and 2. These results are benchmarked with results derived from the same LP model used to generate data. In order to highlight the importance of the constraint imposing model in this work, results are plotted for two cases: IL with constraints, and IL without constraints.

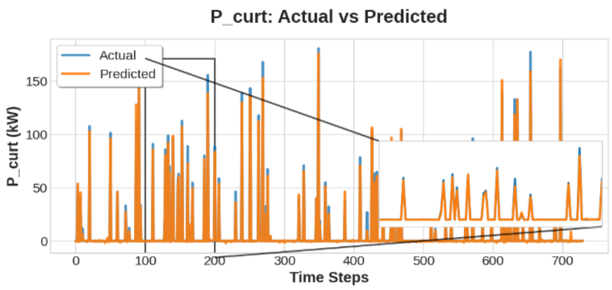

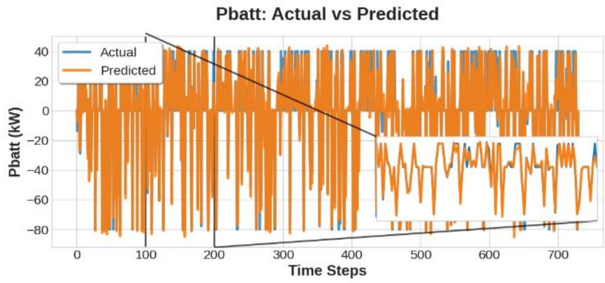

Fig. 6. Predicted and real values for the test dataset.

A typical study day begins with low power demand and low photovoltaic (PV) power generation. In the first test scenario, the battery starts charging during the off-peak period, taking advantage of the low electricity prices in preparation for the anticipated peak demand later in the day. During the mid-peak period, the battery discharges, relying on the peak PV power generated around midday to meet the load requirements during the peak period and to prepare for absorbing excess power. However, when using the IL-based controller, the battery is not fully discharged during this period, which limits its ability to charge later and results in increased curtailed power.

In the second test scenario, the overall performance of the proposed approach closely aligns with the LP trends. The battery charges during low prices and discharges during high-price periods and when PV power is insufficient to cover the load demand. In this case, where PV power is low, the generated PV power is locally consumed. Thus, the storage system charges only during off-peak and mid-peak periods and discharges during the peak period to reduce reliance on the power grid during high-price intervals. Notably, no power is injected into the external grid, and all constraints are maintained, demonstrating the effectiveness of the constraints-enforcement module in enhancing the proposed approach.

In this work, the LP and IL approaches are compared with a focus on energy cost, PV self-consumption rate (α_{sc}), and the grid dependence rate (GDR). Since there is no grid export, α_{sc} and GDR are computed as follow:

$$\alpha_{sc} = \frac{\sum_{t=1}^{24}(P_{PV}(t)-P_{curt}(t))*100}{\sum_{t=1}^{24} P_{PV}(t)} \tag{11}$$

$$GDR = \frac{\sum_{t=1}^{24} P_g(t)*100}{\sum_{t=1}^{24} P_{load}(t)} \tag{12}$$

The proposed approach demonstrates strong performance in maintaining the MG within operational constraints and reducing dependency on the grid. However, In the first test scenario, the global energy cost imported from the utility grid is higher compared to the LP benchmark. On the other hand, the PV self-consumption rate is 6% lower and the GDR is 4% higher compared to LP, these results show a performance gap and suggests further improvement of the model. In contrast, in the second scenario, the operational cost, PV self-consumption rate and the GDR rate closely aligns with LP.

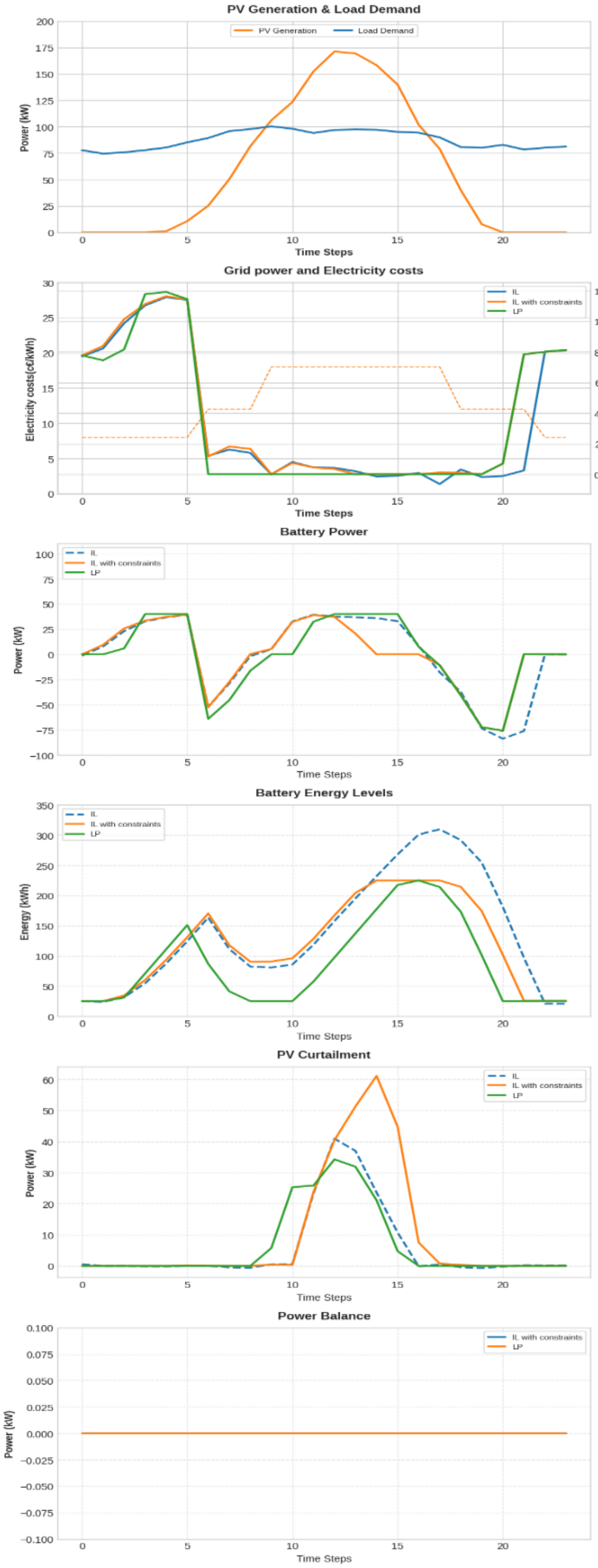

Fig. 7. Comparison of LP-based and IL-based EMS Strategies under Scenario 1.

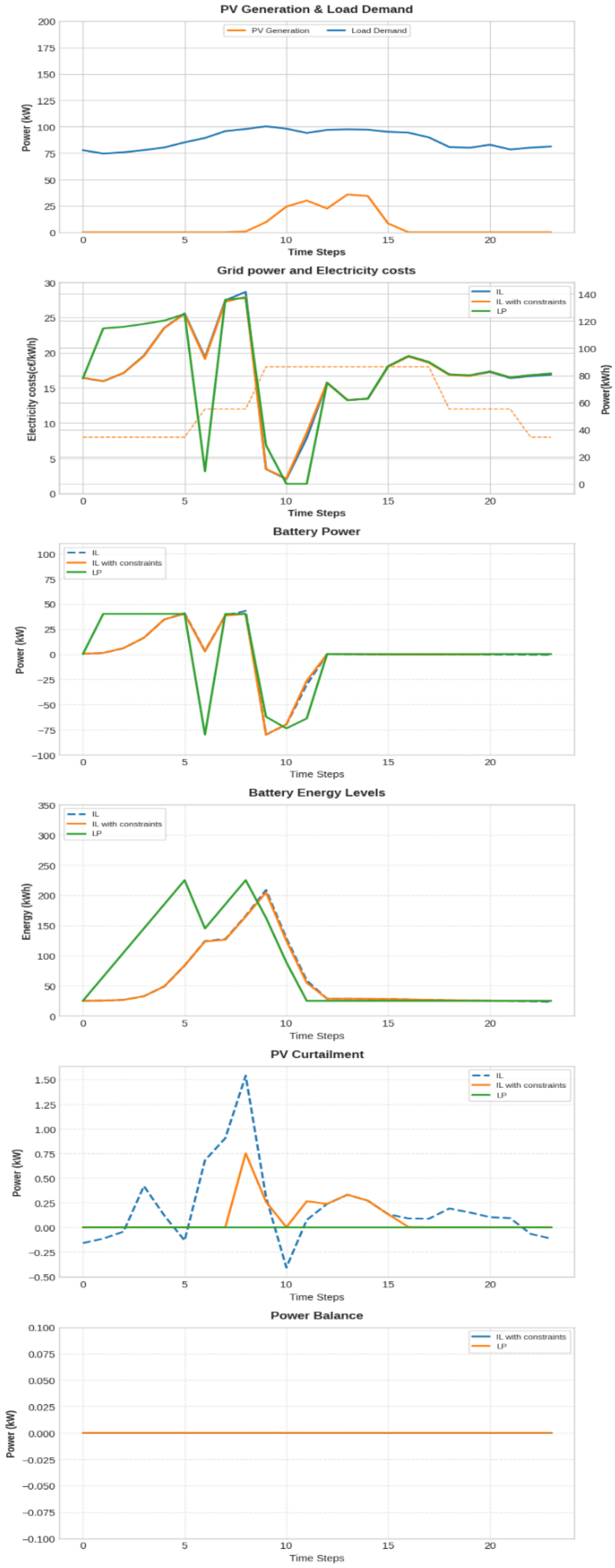

Fig. 8. Comparison of LP-based and IL-based EMS Strategies under Scenario 2.

Table 3. Energy cost, PV self-consumption and grid dependence rates.

Period	LP		IL with constraints
Scenario 1	Cost	70.01 €	80.12 €
	α_{sc}	89%	83%
	GDR	39%	43%
Scenario 2	Cost	228.81 €	232.82 €
	α_{sc}	100%	99%
	GDR	92.11%	92.38%

6. CONCLUSIONS

This article presented an energy management approach for a full-scale MG combining IL with a rule-based post-processing module to enforce operational constraints. By using demonstrations derived from LP as training data, a DL model was trained to predict control setpoints in real-time, eliminating the need for predictive forecasting. The rule-based post-processing module ensured the feasibility of the energy management strategy by correcting the control set points to respect the operational constraints. Simulation results demonstrated that the proposed approach achieves near-optimal performance compared to the LP-based method while allowing efficient real-time operation.

IL has shown promising results in microgrid energy management. However, behavioral cloning, as used in this study, cannot inherently maintain the microgrid constraints and requires post-processing to ensure valid outputs. On the other hand, this approach is dependent on large amounts of high-quality expert demonstration data. Moreover, it may suffer from poor generalization when exposed to unseen data or shifts in system states, which limits its adaptability to changing operational conditions.

Regarding future developments, this approach can be improved by expanding the training dataset to enhance the model's generalization. Additionally, emerging breakthroughs in DL could lead to the development of more advanced models capable of extracting maximum feature information from time-series data. Architectures that integrate domain knowledge, such as physics-informed neural networks, can eliminate the need for post-processing modules to enforce constraints by embedding them directly into the DL model. Finally, testing this approach on a physical system would evaluate its effectiveness under real-world uncertainties.

ACKNOWLEDGEMENTS

Princess Nourah bint Abdulrahman University Researchers Supporting Project number (PNURSP2026R831), Princess Nourah bint Abdulrahman University, Riyadh, Saudi Arabia

The authors acknowledge JUNIA School of Engineering, Lille, France, for providing the data used in this study.

REFERENCES

Ahmadifar, A., Ginocchi, M., Golla, M.S., Ponci, F. and Monti, A. (2023). Development of an Energy Management System for a Renewable Energy Community and Performance Analysis via Global Sensitivity Analysis. *IEEE Access*, 11 (1), 45212-45226.

Aouad, A., Almaksour, K. and Abbes, D. (2024). Storage management optimization based on electrical consumption and production forecast in a photovoltaic system. *Mathematics and Computers in Simulation*, 224.

Aslam, S., Herodotou, H., Mohsin, S.M., Javaid, N., Ashraf, N. and Aslam, S. (2021). A survey on deep learning methods for power load and renewable energy forecasting in smart microgrids. *Renewable and Sustainable Energy Reviews*, 144.

Boato, B., Sueldo, C.S., Avila, L. and De Paula, M. (2023). An improved Soft Actor-Critic strategy for optimal energy management. *IEEE Latin America Transactions*, 21 (9), 1018-1026.

Boralessa, M.A.K.S., Hovden, S., Wickramarathna, A.V.U.A. and Hemapala, K.T.M.U. (2022). Effect of Renewable Energy Forecasting Error on Model Predictive Control Based Microgrid Energy Management System. In *2022 IEEE IAS Global Conference on Emerging Technologies (GlobConET)*, pp. 876-881. IEEE, Arad, Romania.

Brahmendra Kumar, G.V. and Palanisamy, K. (2019). Large scale renewable energy integration: Issues and solutions. *Energies*, 12 (10), 1996.

Chen, L., Wu, P., Chitta, K., Jaeger, B., Geiger, A. and Li, H. (2024). End-to-end Autonomous Driving: Challenges and Frontiers. *IEEE Transactions on Pattern Analysis and Machine Intelligence. 46(12), pp.10164-10183.*

Erdiwansyah, F., Mahidin, F., Husin, H., Nasaruddin, F., Zaki, M., & Muhibbuddin, F. (2021). A critical review of the integration of renewable energy sources with various technologies. *Protection and control of modern power systems*, *6*(1), 3.

Gao, S., bin Zulkifli Lee, R., Huang, Z., Xiang, C., Yu, M., Tan, K. T., & Lee, T. H. (2023). A hybrid approach for home energy management with imitation learning and online optimization. *IEEE Transactions on Industrial Informatics*, *20*(3), 4527-4539.

Hong, T., Pinson, P., Wang, Y., Weron, R., Yang, D., & Zareipour, H. (2020). Energy forecasting: A review and outlook. *IEEE Open Access Journal of Power and Energy*, *7*, 376-388.

Hanley, M., & Ilic, J. (2011). *Frequency instability problems in North American interconnections* (No. DOE/NETL--2011/1473). National Energy Technology Laboratory (NETL), Pittsburgh, PA, Morgantown, WV, and Albany, OR (United States).

Ji, Y., Wang, J., Xu, J., Fang, X., & Zhang, H. (2019). Real-time energy management of a microgrid using deep reinforcement learning. *Energies*, *12*(12), 2291.

Kim, S. H., & Shin, Y. J. (2023). Optimize the operating range for improving the cycle life of battery energy storage systems under uncertainty by managing the depth of discharge. *Journal of Energy Storage*, *73*, 109144.

Kruse, J., Schäfer, B., & Witthaut, D. (2021). Revealing drivers and risks for power grid frequency stability with explainable AI. *Patterns*, *2*(11).

Mystakidis, A., Koukaras, P., Tsalikidis, N., Ioannidis, D., & Tjortjis, C. (2024). Energy forecasting: A comprehensive review of techniques and technologies. *Energies*, *17*(7), 1662.

Ouyang, D., Weng, J., Chen, M., Wang, J., & Wang, Z. (2022). Sensitivities of lithium-ion batteries with different capacities to overcharge/over-discharge. *Journal of Energy Storage*, *52*, 104997.

Swibki, T., Ben Salem, I., Kraiem, Y., Abbes, D., & El Amraoui, L. (2023). Imitation learning-based energy management algorithm: Lille catholic university smart grid demonstrator case study. *Electronics*, *12*(24), 5048.

Sun, H., Zhang, B., & Liu, N. (2024). Imitation learning-based online optimal scheduling for microgrids: An approach integrating input clustering and output classification. *IET Renewable Power Generation*, *18*(15), 3161-3172.

Uddin, M., Mo, H., Dong, D., Elsawah, S., Zhu, J., & Guerrero, J. M. (2023). Microgrids: A review, outstanding issues and future trends. *Energy Strategy Reviews*, *49*, 101127.

U.S. Energy Information Administration (EIA). (n.d.). Electricity explained. U.S. Department of Energy, Washington, D.C. Retrieved April 25, 2025, from https://www.eia.gov/energyexplained/electricity/

Vinothine, S., Widanagama Arachchige, L. N., Rajapakse, A. D., & Kaluthanthrige, R. (2022). Microgrid energy management and methods for managing forecast uncertainties. *Energies*, *15*(22), 8525.

Wang, J., & Azam, W. (2024). Natural resource scarcity, fossil fuel energy consumption, and total greenhouse gas emissions in top emitting countries. *Geoscience frontiers*, *15*(2), 101757.

Zhou, Y., & Ho, C. N. M. (2016, May). A review on microgrid architectures and control methods. In *2016 IEEE 8th international power electronics and motion control conference (IPEMC-ECCE Asia)* (pp. 3149-3156). IEEE.

Zare, M., Kebria, P. M., Khosravi, A., & Nahavandi, S. (2024). A survey of imitation learning: Algorithms, recent developments, and challenges. *IEEE Transactions on Cybernetics*, *54*(12), 7173-7186.